Adaptive Strategy-Enhanced NSGA-II for Multi-Objective Optimization with Improved Convergence and Diversity Control

Yinghui Zhao
School of Artificial Intelligence, Hebi Polytechnic, Hebi 438000, China
E-mail: zhaoyinghui0519@163.com

In modern society, sustainability has become an increasingly important issue. By solving multi-objective problems, decision-makers can make more sustainable decisions. To efficiently solve multi-objective problems, an adaptive strategy is proposed to optimize the crossover and mutation operators of the non-dominated sorting genetic algorithm II (NSGA-II). Moreover, the multi-objective flexible job shop scheduling problem is modeled by incorporating worker fatigue factors. Finally, the algorithm performance was tested using ZDT and DTLZ series test functions, and the multi-objective solving performance of the algorithm was tested based on standard examples FMk01-FMk06. The results showed that in the ZDT1 and ZDT2 test functions, the solution set coverage of the proposed algorithm was 0.833 and 0.906, respectively, and the inverse generation distance was 0.006 and 0.0059, respectively, achieving better convergence and diversity. In the DTLZ1 test function, the inverse generation distance of the proposed algorithm did not exceed 2. In the FMk03 example, the inverse generation distance of the proposed algorithm was 0.009, which was lower than the traditional NSGA-II algorithm. In the FMk06 example, the proposed algorithm achieved a super volume of 0.37, which was higher than the multi-objective squirrel search algorithm and NSGA-III algorithm. The experiment has demonstrated the effectiveness of the improved algorithm in solving multi-objective issues. The research results contribute to improving the efficiency of addressing multi-objective optimization and complex problems in real life, enhancing the scientificity and effectiveness of decision-making.

Povzetek: Prispevek predlaga izboljšano različico NSGA-II z adaptivnimi operaterji v normalno porazdelitvijo za učinkovitejše reševanje večciljnih optimizacij, vključujoč tudi modeliranje utrujenosti delavcev.

1 Introduction

The deepening of globalization has made the problems faced by modern society increasingly complex. The competition among enterprises is no longer a simple product competition, but a competition of their comprehensive strength. Multi-Objective Problem (MOP) is closely related to modern development, referring to the problem of simultaneously considering multiple objective functions in the optimization process. It can help decision-makers balance the relationships between multiple objectives and achieve comprehensive optimization [1-2]. Sharma S et al. explored the advantages and disadvantages of Multi-Objective Optimization (MOO) algorithms and their variants, and discussed the challenges faced by various multi-objective algorithms in engineering applications. This study helped to expand the application scope of MOO algorithms [3]. Deng W et al. proposed a fast Non-dominated Sorting Genetic Algorithm II (NSGA-II) based on Adaptive Crossover (AC) strategy, and improved the selection strategy using a special congestion strategy. The algorithm could find the global Pareto solution set [4]. Jangir P et al. designed a multiple objective marine predator algorithm built on Elite Non-Dominated Sorting (NDS) and Crowding Distance

Mechanism (CDM) and tested it based on Pareto front problems. This algorithm had good performance in solving MOPs [5]. Sharma S et al. constructed a Butterfly Optimization Algorithm based on dominance sorting and CDM to address the MOP. This algorithm had good application effects in solving various discrete, continuous, linear, and nonlinear characteristic problems based on the Pareto front, and had a fast convergence speed [6]. Liu et al. addressed the challenge of mapping IoT applications to fog units and modeled the fog service layout issue as an MOP, using an evolutionary algorithm based on cuckoo search to solve it. The method could effectively reduce energy consumption and service latency [7]. Ali A et al. put forward a single and multiple objective hybrid scheme that fuses parameter-free constraint techniques to find Pareto fronts with better convergence and uniform distribution for the problem of high cost and computational complexity in optimal power flow. This method could find the near global Pareto front of highly complex issues while meeting constraints [8].

The NSGA-II adopts a fast Non-Dominated Sorting (NDS) algorithm to reduce computational complexity and has significant advantages and wide applications in MOP solving [9]. Chen L et al. compared the relationship between aspect ratio and maximum temperature

difference based on heat transfer theory for multi-objective structural design of quadrilateral heating elements, and solved for the optimal aspect ratio using NSGA-II. The maximum temperature difference of the optimal construction decreased by 5.6%, the deviation index of MOO was smaller than that of single objective optimization, and the resulting structure had better comprehensive thermal conductivity [10]. Lv L et al. proposed an NSGA-II inventory scheduling model with a local search for integrated production based on state maintenance, which helps to reduce total delays and total Completion Time (Ctime). This model has demonstrated good optimization scheduling performance in large-scale instances [11]. Jalili A et al. combined SVM and NSGA-II to minimize the decline of groundwater level for the MOO scheduling problem of reservoirs. The mean error rate of the proposed method was less than 2.5%, which could provide the best operating strategy based on new data on dam inflow [12]. Singh M K et al. proposed a hybrid data routing protocol for optimizing the flight trajectory of drones in Wireless Sensor Networks (WSN) and utilized the NSGA-II for optimization to reduce UAV energy consumption. This method could improve the network lifetime and network throughput of WSN [13]. Chen L et al. modeled the energy scheduling in steel manufacturing as a multiple objective vehicle routing issue and developed an NSGA-II grounded on the knowledge. The spacing indicator of this algorithm decreased by about 40%, and the overcapacity indicator increased by about 57% [14]. Wang J et al. put forth a novel MOO method for the design of printed circuit heat exchangers. It obtained three optimization design variables through dimensionless wing fin arrangement parameters and used NSGA-II to construct a Pareto optimal frontier. This method could meet the requirements of high heat transfer performance and low flow resistance [15]. The summary table of the above literature is shown in Table 1.

In summary, although many scholars have extensively researched MOP in the past and affirmed the NSGA-II performance in addressing MOPs, traditional NSGA-II algorithms still suffer from the problem of easily getting stuck in local optima. Therefore, this paper will propose an improved NSGA-II algorithm on the basis of Adaptive strategy (ANSGA-II). The study aims to propose effective strategies to improve the application effectiveness of NSGA-II in solving MOP, thereby better adapting to the needs of complex problems. The innovation lies in utilizing adaptive strategies to optimize crossover and mutation operators, thereby strengthening the global search ability.

The main contribution of this study is: (1) The ANSGA-II algorithm that can dynamically adjust operating parameters according to environmental changes is proposed, which can improve the convergence speed of the algorithm and the diversity of its solutions. (2) A crossover operator based on normal distribution is introduced to replace the original simulated binary crossover operator, which can enhance the algorithm's spatial search capability and avoid local optima. (3) The worker fatigue factors are incorporated into the modeling of multi-objective Flexible Job Shop Scheduling (FJSS) problems, which can more accurately reflect the actual situation and provide a more realistic optimization model for actual production scheduling.

Table 1: Literature summary table.

Literature	Algorithm	Performance index	Application area	Limitation
Deng W [4]	Enhanced Fast NSGA-II	Global Pareto solution set	Engineering field	High computational complexity and sensitivity to parameters
Jangir P [5]	Multi-target ocean predator algorithm	Global Pareto solution set	Constraints and Engineering Design	Slow convergence speed and low solution accuracy
Sharma S [6]	Butterfly Optimization Algorithm	Convergence speed	MOO	Possible increase in computational complexity
Liu C [7]	Cuckoo search algorithm	Energy consumption and service delay	IoT applications	Fog service layout issue
Ali A [8]	Single objective and multi-objective hybrid algorithm	Global Pareto solution set	Optimal Trend Problem	Possible increase in computational complexity
Chen L [10]	NSGA-II	Maximum temperature difference	Multi-objective structural design of quadrilateral heating element	High computational complexity and sensitivity to parameters
Lv L [11]	NSGA-II with Local Search	Total delay and total Ctime	Inventory scheduling	May exhibit instability in dynamic environments
Jalili A A [12]	SVM and NSGA-II	Average error rate	Multi objective optimization scheduling of reservoirs	Possible increase in computational complexity
Singh M K [13]	Multi-objective NSGA-II	Energy consumption	WSN	Possible increase in computational complexity
Chen L [14]	Knowledge based NSGA-II	Ultra Capacity	Energy dispatch	Difficulty maintaining diversity in high-dimensional problems

Wang J [15]	NSGA-II	Heat transfer performance	Heat Exchanger Design	Difficulty maintaining diversity in high-dimensional problems

2　Methods and materials

To better solve MOP, an ANSGA-II algorithm will be proposed, and a multi-objective FJSS problem will be modeled by combining worker fatigue factors to verify the effectiveness of ANSGA-II in solving MOP.

2.1　NSGA-II algorithm based on adaptive strategy

NSGA-II is a classic MOO algorithm developed on the basis of NSGA, which fully utilizes the relationships between individuals and selects the Pareto Optimal Solution (POS) set through NDS and crowding distance calculation. NSGA-II exhibits superior convergence speed and solutionquality [16]. The process of the traditional NSGA-II is displayed in Figure 1.

In Figure 1, the basic steps of NSGA-II include initializing the population, calculating fitness values, NDS, calculation of crowding distance, selection operation, crossover operation, and mutation operation, as well as the introduction of fast NDS, crowding distance, and Elite Retention Strategy (ERS). Fast NDS is mainly used to classify a solution set according to non-dominated relationships. NDS is taken to evaluate the pros and cons of different solutions in MOO. If a solution outperforms another solution on all objectives, it is said to dominate the other solution [17]. If there is no solution that dominates the other solution, then these two solutions are called non-dominated solutions. The NSGA-II's crowding distance is an indicator for evaluating the distribution density of individuals in a population. The larger the crowding distance, the more dispersed the distribution of individuals, which is used to keep population diversity in MOO problems. The formula of crowding distance d_i is shown in equation (1).

$$d_i = \sum_{o=1}^{a} \left(\left| f_o^{l+1} - f_o^{l-1} \right| \right), o = 1, 2, ..., a \qquad (1)$$

In equation (1), a is the amount of objective functions. f_o^{l+1} and f_o^{l-1} are the function values of individual $l+1$ and $l-1$ on the o-th objective. The ERS of NSGA-II refers to the selection of individuals through Pareto non-dominated levels and crowding distances after merging parent and offspring populations. This is done to ensure that excellent individuals are not eliminated, thereby maintaining population diversity and optimizing the accuracy of results [18]. Figure 2 shows the ERS process.
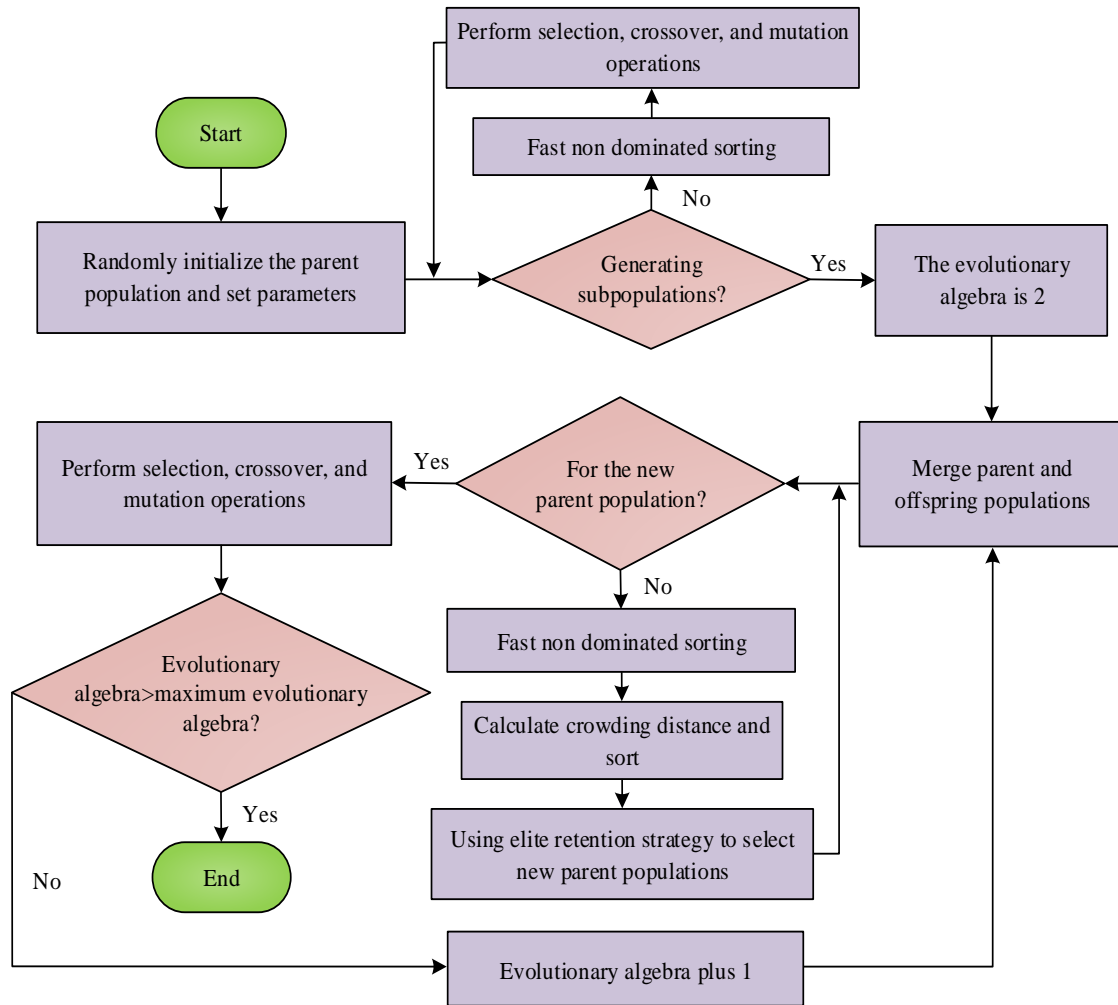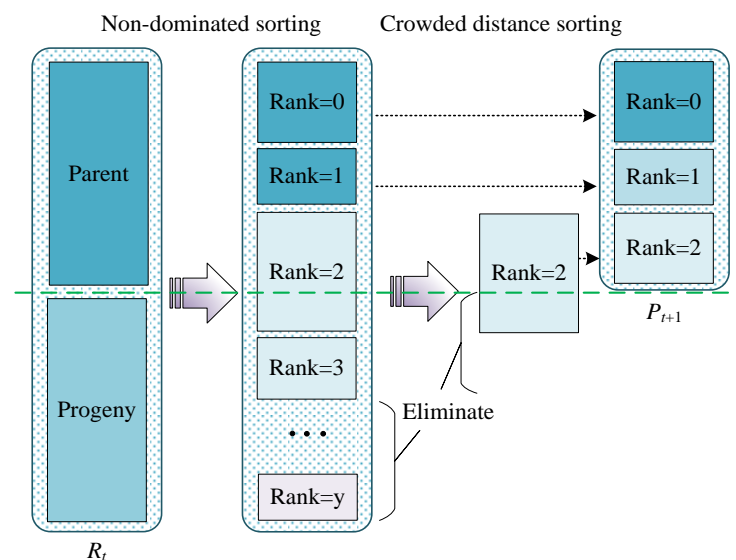
Figure 1: The flowchart of NSGA-II.

Figure 2: Schematic diagram of elite retention strategy.

In Figure 2, all individuals of the parent and child generations form population R_t, with a scale of $2N$. In R_t, selecting N from individuals based on NDS and crowding order can form a new next-generation population p_{t+1}. In NSGA-II, the crossover probability determines the probability of the parent individual being selected in the crossover operation. A low crossover probability may lead to insufficient population diversity, while a high crossover probability may result in premature convergence of the population to a local optimum. The

probability of mutation is utilized to lift the population diversity. A low mutation rate may lead to insufficient diversity in the population, making the algorithm prone to jumping into local optima, while a high mutation rate may cause the population to be too dispersed and hard to converge to the global optimum [19]. The crossover probability and mutation probability of the traditional NSGA-II algorithm are fixed and cannot adapt to different optimization problems. This fixity limits the global search capability of the algorithm, especially when facing complex MOPs, which may lead to the algorithm getting stuck in local optima and unable to effectively explore the solution space. Therefore, this study proposes to use adaptive strategies to optimize crossover and mutation operators to perfect the optimization performance. In the early stages of evolution, a higher probability of crossover and mutation helps to expand the search range and avoid premature convergence. In the later stages of evolution, smaller crossover and mutation probabilities help with fine search, improving the quality and accuracy of solutions. By introducing adaptive parameters, the crossover probability and mutation probability can be dynamically adjusted according to the evolutionary state of the population, thereby improving the global search capability of the algorithm [20]. The improved crossover probability C is given by equation (2).

$$C = \varepsilon - \frac{2e^{-(n/T)}}{1+e^{-(n/T)}} c \qquad (2)$$

In equation (2), ε is the adaptive parameter. c is the fixed crossover probability. n is the quantity of iterations. T means the maximum n. The improved mutation probability V is shown in equation (3).

$$V = \frac{2e^{-(n/T)}}{1+e^{-(n/T)}} v \qquad (3)$$

In equation (3), v is the given mutation probability. In addition, the traditional NSGA-II crosses the parental chromosomes by simulating the single point crossing method in binary encoding. The expression for simulating binary crossover method is shown in equation (4).

$$\begin{cases} c_{1,i} = \dfrac{(1+\beta)p_{1,i} + (1-\beta)p_{2,i}}{2} \\ c_{2,i} = \dfrac{(1-\beta)p_{1,i} + (1+\beta)p_{2,i}}{2} \end{cases} \qquad (4)$$

In equation (4), c_1 and c_2 are the offspring chromosomes, β is a random variable, and p_1 and p_2 are the parent chromosomes. The calculation of β is shown in equation (5).

$$\begin{cases} \beta = (\dfrac{1}{2-2rand})^{1/(1+\eta)}, rand > 0.5 \\ \beta = (2rand)^{1/(1+\eta)}, rand \le 0.5 \end{cases} \qquad (5)$$

In equation (5), η is a constant and *rand* is a random number within [0, 1]. After integration, the simulated binary crossover method can be expressed as equation (6).

$$c_{1/2} = \frac{\left(p_{1,i}+p_{2,i}\right)}{2} \pm \beta \frac{\left(p_{1,i}-p_{2,i}\right)}{2} \qquad (6)$$

However, the global search capability of this simulated binary crossover method is poor, especially in multi-modal MOPs, which may not effectively explore the decision space. Therefore, this study proposes a crossover operator based on normal distribution. The introduced evolutionary strategy is given by equation (7).

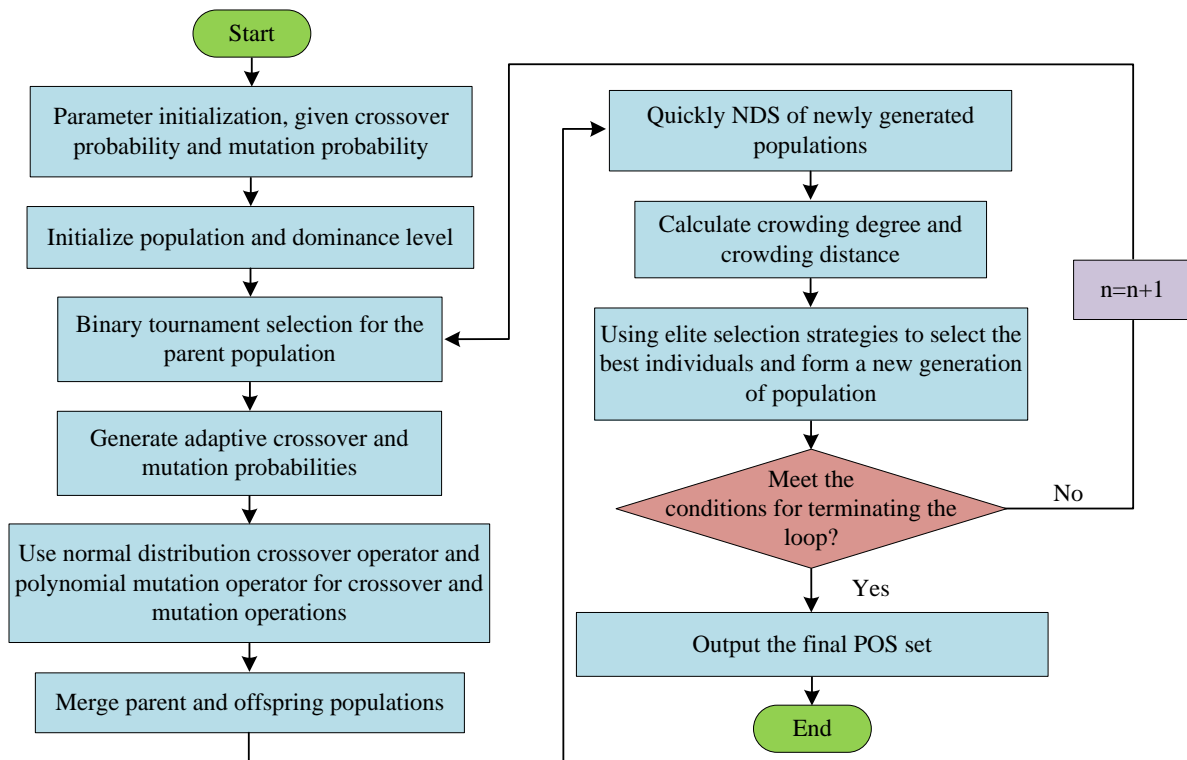$$x' = x + \sigma \times N(0,1) \qquad (7)$$

Figure 3: Process diagram for improved NSGA-II algorithm.

In equation (7), x' is a new individual, σ is the search step size, x is an old individual, and $N(0,1)$ means a random variable that follows a normal distribution. To apply the normal distribution in the crossover operator, this study takes $\dfrac{(p_{1,i} - p_{2,i})}{2}$ as the search step size, and the improved crossover operator is shown in equation (8).

$$c_{1/2} = \frac{(p_{1,i} + p_{2,i})}{2} \pm 1.481 \frac{(p_{1,i} - p_{2,i})}{2} \cdot |N(0,1)| \quad (8)$$

The process of the ANSGA-II algorithm is displayed in Figure 3.

In Figure 3, ANSGA-II introduces AC probability and mutation probability, combined with normal distribution crossover operator, helping improve the optimization performance and avoid falling into local optima.

2.2   MOP solution based on ANSGA-II

After proposing the ANSGA-II algorithm, to further verify its performance in MOP solving, this study models a classic MOP, namely FJSS. Taking FJSS as an example, the performance of ANSGA-II in MOP solving is verified. The FJSS issue involves processing n workpiece on m devices [21]. Each workpiece has 1 or 1+ processes. The sequence is fixed, and each process is able to be processed on multiple various processing equipment. The processing period of each process changes with the different processing machines. The scheduling objective is to choose the best equipment for each process, decide the

superior processing sequence and beginning time on each equipment, and perform the best indicators such as Ctime, total load, etc. for the entire system [22]. The structure of the FJSS problem is shown in Figure 4.

The traditional FJSS problem model only considers equipment constraints and ignores worker participation in workshop production [23]. Therefore, the multi-objective FJSS problem model established further considers the worker factor on the basis of common optimization objectives, with the optimization objectives of minimizing error costs, maximum Ctime, Total Energy Consumption (TEC), and overall equipment load. Assuming there are m devices with a set of $M = \{M_1, M_2, ..., M_M\}$, w workers with a set of $W = \{W_1, W_2, ..., W_w\}$, and n workpieces with a $J = \{J_1, J_2, ..., J_n\}$. Each workpiece J_i needs toundergo r processing steps, and the set of processes is $O = \{O_{i1}, O_{i2}, ..., O_{ir}\}$. There is a constraint on the order of processes for the same workpiece. Through problem analysis, this study decomposes the solution of FJSS problem into three sub problems: equipment selection, worker allocation, and process sequencing. Before modeling, this study also makes the following assumptions: all processes can only be stopped once they are completed; All workpieces can be processed at the beginning; All processes require the participation of equipment and workers; Neglecting the time spent transferring workpieces across different devices; The same equipment cannot process multiple processes simultaneously (applicable to single core equipment or equipment with limited resources); The same worker
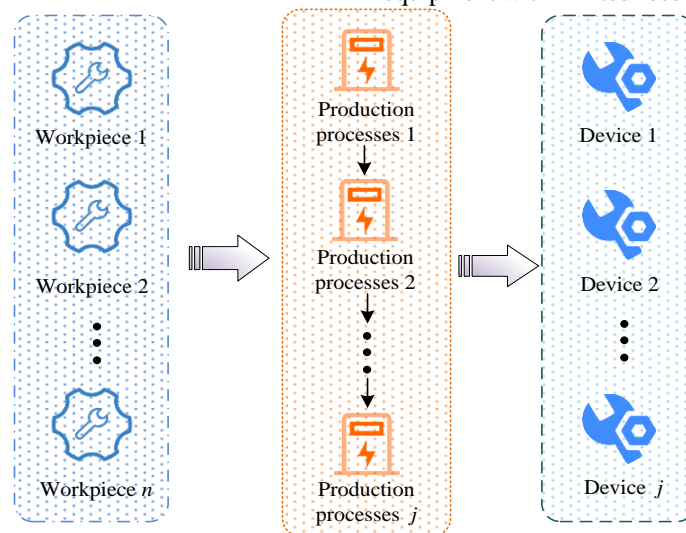

Figure 4: Schematic diagram of flexible workshop scheduling problem.

cannot operate multiple devices simultaneously; Workers can rest during their free time. The maximum Ctime $C_{\max}$ is the length of time from the first process of processing the first workpiece to the completion of the last process of processing the last workpiece. By minimizing the maximum Ctime, waiting time and resource idle can be reduced, thereby improving overall production efficiency. The objective function f_1 for minimizing the maximum Ctime is shown in equation (9).

$$f_1 = \min C_{\max} = \min \{C_i, i \in n\} \quad (9)$$

In equation (9), C_i is the final Ctime of workpiece J_i. The total load of equipment refers to the total workload that the equipment bears during operation. By minimizing the total load of the equipment, the service life of the equipment can be extended. The function f_2 that minimizes the total load of the equipment is shown in equation (10).

$$f_2 = \min\left(\sum_{i=1}^{n}\sum_{j=1}^{r_i}\sum_{k=1}^{m} T_{ijk} x_{ijk}\right) \quad (10)$$

In equation (10), T_{ijk} is the time required for equipment M_k to process process O_{ij}. If equipment M_k processes process O_{ij}, the value of x_{ijk} is 1, otherwise it is 0. TEC is the gross of energy consumed by all workpieces in all processes during the production process. The TEC E in FJSS is mainly composed of the energy consumption E_k^p during equipment operation, the energy

consumption E_k^n when the equipment is unloaded, and the fixed energy consumption E_f in the workshop. Its calculation is shown in equation (11).

$$\begin{cases} E_k^p = \sum_{i=1}^{n}\sum_{j=1}^{r_i}\left(T_{ijk} x_{ijk}\right) p_{ijk}^p \\ E_k^n = \left[TM_k - \sum_{i=1}^{n}\sum_{j=1}^{r_i}(T_{ijk} x_{ijk})\right] p_k^n \\ E_f = \left(\max C_i\right) p_f \\ E = \sum_{k=1}^{m}\left(E_k^p + E_k^n\right) + E_f \end{cases} \quad (11)$$
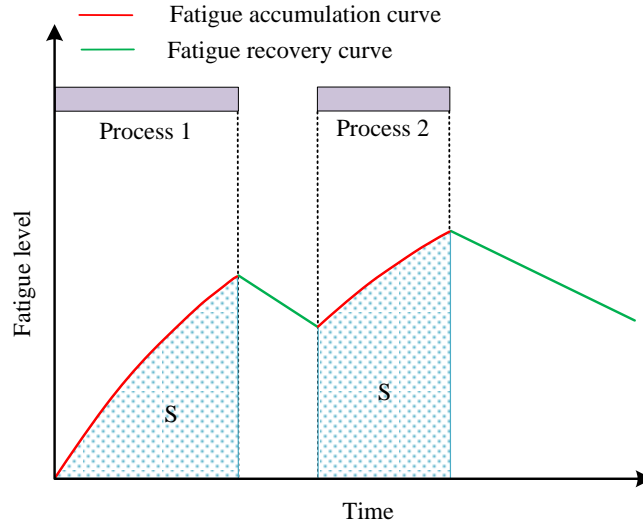

Figure 5: Changes in workers' fatigue levels.

In equation (11), p_{ijk}^p is the processing power of process O_{ij} on equipment M_k. TM_k is the Ctime of the last process on device M_k. p_k^n is the no-load power of device M_k. p_f is the fixed power of the workshop unit. Minimizing TEC refers to optimizing energy usage and management strategies under specific conditions to minimize the TEC of a system or equipment. The function f_3 that minimizes the TEC is shown in equation (12).

$$f_3 = \min\left[\sum_{k=1}^{m}\left(E_k^p + E_k^n\right) + E_f\right] \quad (12)$$

Error cost refers to the decrease in operational accuracy of workers due to fatigue when operating equipment, which in turn affects the quality of the product. In practical situations, as working hours increase, the fatigue level of workers will gradually increase, and the fatigue level during rest will gradually decrease. The changes in workers' fatigue levels are shown in Figure 5.

In Figure 5, S is the area enclosed by the fatigue curve. The fatigue level of workers will increase with the increase of working hours and decrease with the increase of rest time [24]. The impact of worker fatigue level on error rate is shown in equation (13).

$$\log_{10}(HEP_{lt}) = 6\log_{10}\left[\frac{FW_l(t)}{F_{mac}}\beta\right], 0 < \beta \le 1 \quad (13)$$

In equation (13), HEP_{lt} is the error rate of worker l at time t. $FW_l(t)$ is the fatigue level of l at t. $F_{\max}$ is

the maximum level of fatigue for workers. β is a constant. Among them, $F_{\max}$ is determined through experiments and data analysis. Fatigue tests are conducted on workers to find the upper limit of fatigue, while their fatigue levels under different working and resting conditions are recorded. The calculation of $FW_l(t)$ is shown in equation (14).

$$FW_l(t) = FW_l(t_1)e^{-\mu(t-t_1)}, 0 \le t_1 \le t, \mu \ge 0 \quad (14)$$

In equation (14), μ represents the fatigue recovery coefficient, which is determined by the characteristic coefficient of the worker, and its calculation is shown in equation (15).

$$\mu = (\delta - rw_l)\gamma \quad (15)$$

In equation (15), δ and γ represent normal numbers. rw_l represents the characteristic coefficient of worker l, mainly determined by factors such as age, physical function, and skill level. Considering that the operation of equipment by workers is a continuous process, this study uses the mean fatigue level of workers in a certain process to represent the fatigue level of that process. The expression of fatigue level and error rate is shown in equation (16).

$$\begin{cases} SO_{ijkl} = \int_{t_0}^{t_0 + T_{ijkl}} \left\{ FW_l(t_0) + [1 - FW_l(t_0)][1 - e^{-\lambda(t - t_0)}] \right\} dt \\ FO_{ijkl} = SO_{ijkl} / T_{ijkl} = 1 - [1 - FW_l(t_0)](1 - e^{-\lambda T_{ijkl}}) / (\lambda T_{ijkl}) \quad (16) \\ \log_{10}(HEP_{ijkl}) = 6\log_{10}\left[\dfrac{FO_{ijkl}}{F_{mac}} \beta \right], 0 < \beta \le 1 \end{cases}$$

In equation (16), SO_{ijkl} is the S when worker l operates equipment M_k to process O_{ij}. t_0 is the starting time of the process processing. T_{ijkl} is the time required for worker l to process O_{ij}. FO_{ijkl} and HEP_{ijkl} are the fatigue levels and error rates of worker l when operating equipment M_k and processing process O_{ij}. The function f_4 that minimizes the cost of errors is shown in equation (17).

$$f_4 = \min\left[\sum_{i=1}^{n} \sum_{j=1}^{r_i} \sum_{k=1}^{m} \sum_{l=1}^{w} x_{ijkl} MC_{ijkl} \right] (17)$$

In equation (17), MC_{ijkl} is the error cost incurred by worker l when operating equipment M_k to process process O_{ij}. To solve the FJSS problem, this study adopts a Dual Layer Encoding (DLE) method built on process and equipment, as shown in Figure 6.

In Figure 6, the i-th occurrence of the workpiece number in the process-based coding indicates the i-th machining process corresponding to the workpiece. The number in the device-based encoding represents the process being processed on the selectable k-th machine. The corresponding DLE can be obtained by corresponding up and down. This study adopts a greedy decoding algorithm with simple implementation and fast execution speed to transform chromosomes into solutions in scheduling problems. The greedy decoding algorithm first considers each process in the order encoded in the chromosome and then searches for the earliest available machine to minimize waiting time and maximize machine utilization until all processes are scheduled for processing.
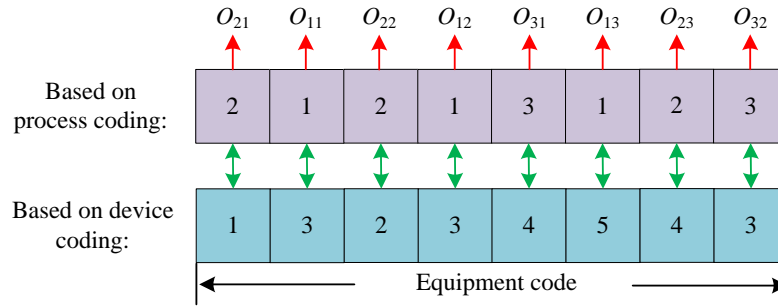

Figure 6: The schematic diagram of double-layer encoding.

3 Results

In the previous text, the study proposed an ANSGA-II algorithm and modeled the multi-objective FJSS problem by combining worker fatigue factors. However, its effectiveness has not been verified yet. Therefore, further analysis of the performance of the proposed ANSGA-II algorithm will be conducted to evaluate its effectiveness in solving MOPs.

3.1 Performance analysis of improving NSGA-II

To test the ANSGA-II performance, this study performs experiments on the Windows 10 operating system with a central processing unit of i7-9800X, 16GB of memory, and MATLAB R2016a software. The experiment is conducted using ZDT and DTLZ series test functions. The crossover and mutation probabilities of the ANSGA-II algorithm are adaptively adjusted based on the number of iterations. In ZDT1-3, the population size is set to 100 and the number of iterations is set to 200. The population size is set to 300 and the iteration count is set to 250 in ZDT6. Inverted Generation Distance (IGD) and Set Coverage Metric (C-metric) are used as evaluation metrics. IGD evaluates the convergence and distribution performance of the algorithm by calculating the minimum distance between each individual on the true Pareto front and the

set of individuals obtained by the algorithm. The smaller the value of IGD, the better the convergence and distribution performance of the algorithm. The C-metric represents the dominance relationship between solutions. When the C-metric (A, B)=1, it indicates that all individuals in B are dominated by at least one individual in A. Typically, the larger the C-metric (A, B), the poorer the convergence of B. The proposed algorithm, traditional NSGA-II algorithm, and Multi-Objective Evolutionary Algorithm based on Decomposition (MOEA/D) algorithm are compared. Due to the randomness of MOO algorithms such as evolutionary algorithms, the results of a single run may not accurately reflect the true performance of the algorithm. Therefore, to control randomness and ensure the reliability of the results, each algorithm is independently run 20 times, and the statistical data are taken as the average of each algorithm. The comparison results of the indicators of the three algorithms are shown in Table 2. In the ZDT1 and ZDT2 test functions, ANSGA-II performs better overall than NSGA-II and MOEA/D about IGD and C-metric. In the ZDT1 and ZDT2 test functions, the proposed algorithm achieves better convergence and diversity with C-metric metrics of 0.833 and 0.906, and IGD metrics of 0.006 and 0.0059, respectively. This indicates that the designed algorithm has good performance in IGD and C-metric, with certain feasibility.

To demonstrate the performance of the designed method more intuitively, the POSs gained by the three algorithms on the ZDT2 test function are compared, as shown in Figure 7. Comparing Figures 7 (a), (b), and (c), the proposed algorithm obtains a high-quality Pareto optimal frontier on the ZDT2 function, which can effectively approximate the true Pareto frontier. There is a significant gap between the POS obtained by MOEA/D and the optimal solution of the ZDT2 function. This indicates that ANSGA-II has high accuracy in solving MOPs.

To verify the computational complexity of the proposed ANSGA-II, the running times of the three algorithms are compared, and the results are shown in Table 3. From Table 3, the running time of ANSGA-II algorithm is higher than MOEA/D but lower than NSGA-II. This indicates that the proposed ANSGA-II algorithm not only improves performance but also reduces computational complexity to a certain extent and improves computational efficiency.

To verify the effectiveness of the improvement strategy, ablation tests are carried out. The NSGA-II, ANSGA-II without AC probability (A), ANSGA-II without improved mutation probability (B), ANSGA-II without adaptive crossover operator (C), and ANSGA-II algorithm without AC and mutation probabilities (D) are compared with the complete ANSGA-II. Figure8 shows the experimental results. In Figure8 (a), in the DTLZ1, as the targets increase, the IGD metrics of all four algorithms show a gradually increasing trend. Among them, the IGD index of the complete ANSGA-II is always the smallest, not exceeding 2. The IGD index of the traditional NSGA-II algorithm is always the highest, followed by the ANSGA-II algorithm without AC and mutation probabilities. In Figure 8 (b), in DTLZ 2, the IGD index of the complete ANSGA-II is still the smallest, not exceeding 1. Therefore, the proposed improvement strategies can well lift the NSGA-II's performance and have certain effectiveness.

Table 2: Comparison results of indicators for three algorithms.

Test function	Index	Algorithm		
		MOEA/D	**NSGA-II**	**ANSGA-II**
ZDT1	IGD	0.0203	0.0101	0.0060
	C-metric	1.0000	0.9775	0.8330
ZDT2	IGD	0.6786	0.0111	0.0059
	C-metric	1.0000	1.0000	0.9060
ZDT3	IGD	0.2060	0.0086	0.0088
	C-metric	1.0000	0.9085	0.8885
ZDT6	IGD	0.0138	0.0172	0.0137
	C-metric	1.0000	1.0000	0.0000

Table 3: Comparison of running time of three algorithms.

Test function	Algorithm		
	MOEA/D	**NSGA-II**	**ANSGA-II**
ZDT1	3.12	9.30	5.31
ZDT2	3.22	12.31	7.90
ZDT3	3.18	15.96	8.44
ZDT6	132.13	2495.22	1488.07

(a) NSGA-II

(b) MOEA/D

(c) ANSGA-II
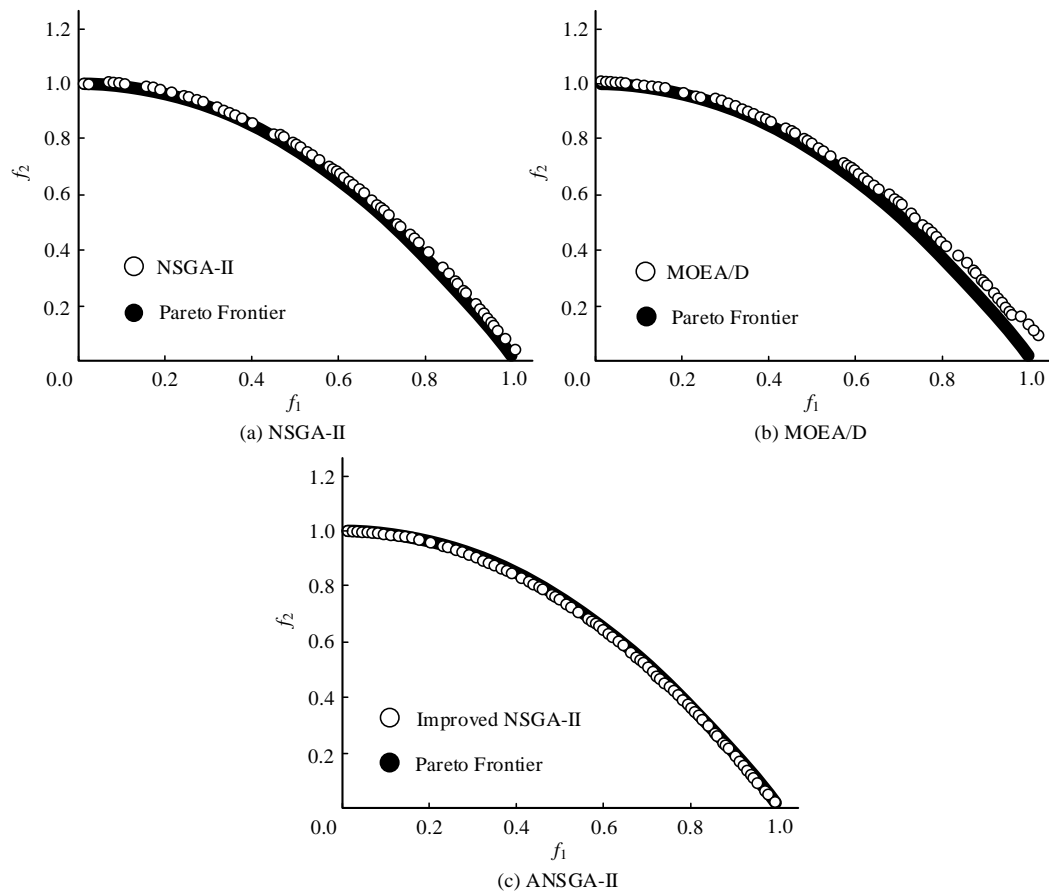
Figure 7: The POS obtained by the algorithm on the ZDT2 test function.

(a) DTLZ1

(b) DTLZ2

Figure 8: Results of ablation experiment.

(a) Comparison of HV indicators   (b) Comparison of IGD indicators
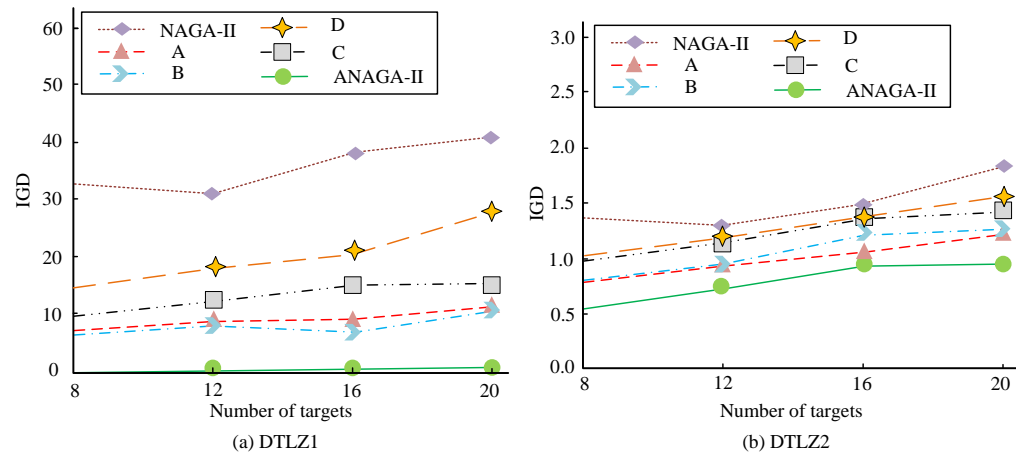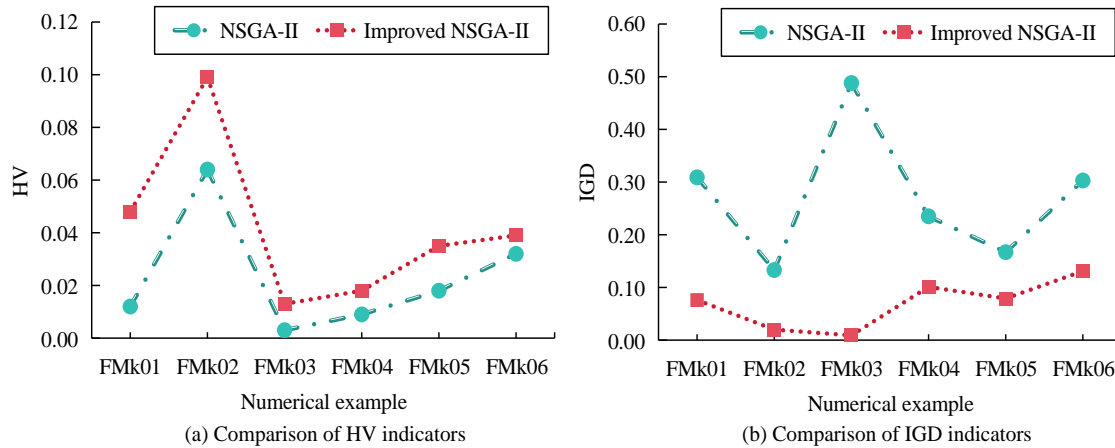
Figure 9: Comparison of HV and IGD indicators between two algorithms.

Table 4: Sensitivity analysis results.

Parameter		Makespan/h	Total energy consumption/kW·h	Error cost/yuan
Fmax	50	100	503	200
	75	104	498	180
	100	108	505	170
γ	0.1	100	503	200
	0.3	94	485	172
	0.5	87	476	161

3.2 Analysis of the effect of MOP solution

Sensitivity analysis is conducted to demonstrate how different fatigue model parameters affect scheduling performance. The maximum fatigue levels are set to 50, 75, and 100, respectively. The fatigue recovery rate is set to 0.1, 0.3, and 0.5. The sensitivity analysis results are shown in Table 4. From Table 4, as the maximum fatigue level increases, the maximum Ctime gradually increases and the error cost gradually decreases. As the fatigue recovery rate increases, the maximum Ctime gradually decreases, and the TEC and error cost both gradually decrease. The sensitivity analysis results indicate that the fatigue model parameters have a significant impact on scheduling performance.

To investigate the application effect of ANSGA-II in MOP solving, a fixed crossover probability of 0.8, a fixed mutation probability of 0.1, a population size of 200, and 150 iterations are set. Based on the standard calculation examples FMk01-FMk06, data such as equipment energy consumption, raw material costs, unit time costs of workers, and unit time costs of equipment have been added. The unit time costs of workers and equipment are 20 yuan/h and 1.2 yuan/kw·h, respectively. The proposed model is compared with NSGA-II using Hypervolume (HV) and IGD as evaluation indicators, as shown in Figure 9. In Figure 9 (a), the HV index of the ANSGA-II is higher than that of NSGA-II in different examples, with the highest HV value of 0.098 in the FMk02 example. In Figure 9 (b), the IGD index of the proposed algorithm is lower than that of the NSGA-II, with the lowest IGD value of 0.009 in the FMk03 example. The ANSGA-II exhibits convergence and distribution, demonstrating good MOP solving performance.
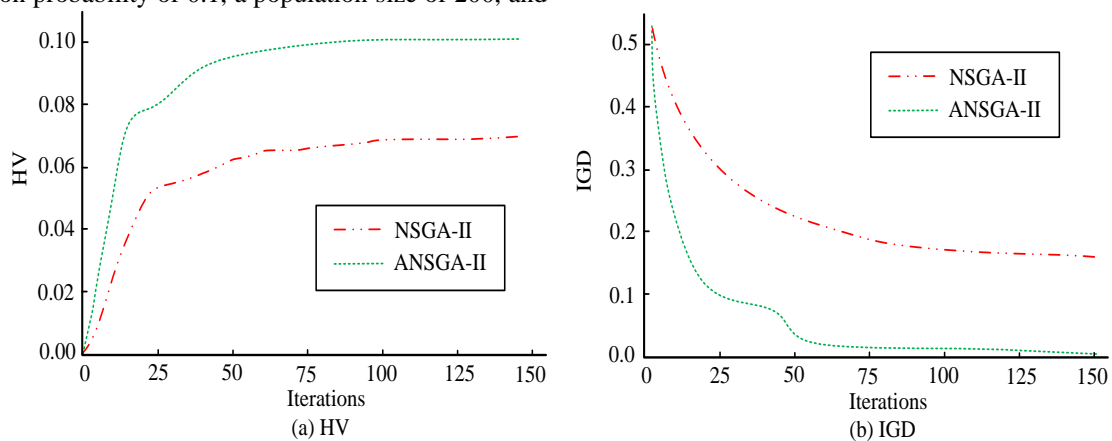

(a) HV   (b) IGD

Figure 10: Comparison of convergence graphs.

(a) Pareto fronts obtained by NSGA-II
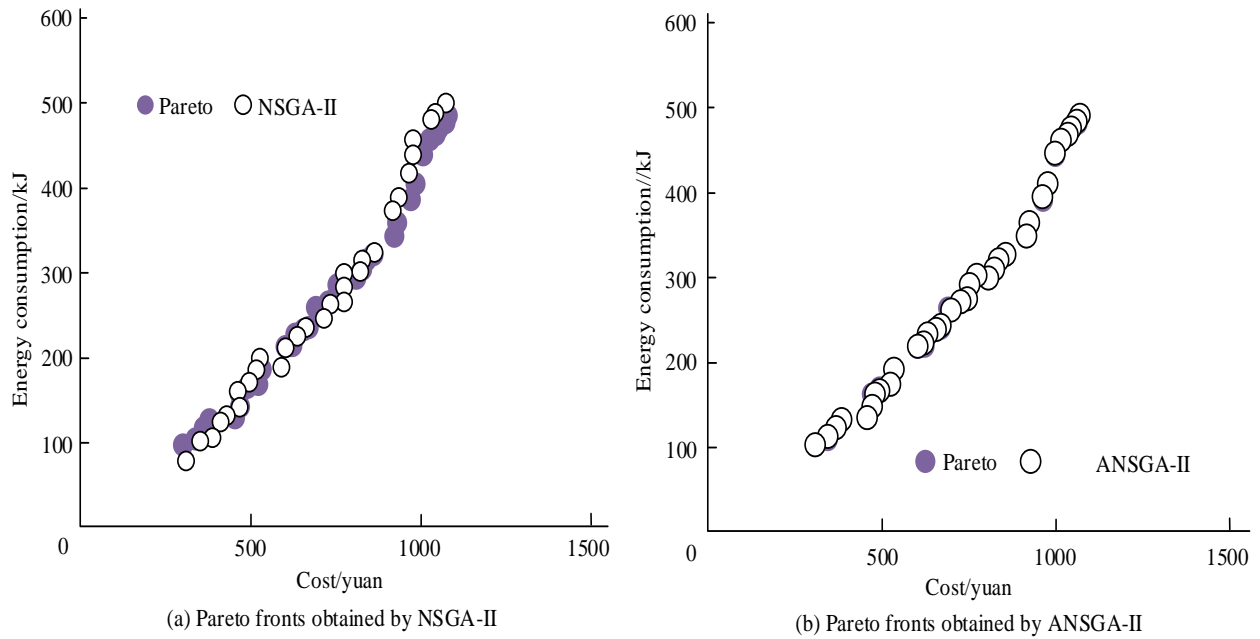
(b) Pareto fronts obtained by ANSGA-II

Figure 11: Pareto frontiers between two algorithms.

To compare the convergence speed of ANSGA-II and NSGA-II, their convergence graphs in the FMk02 example are compared, and the results are shown in Figure 10. Figures 10 (a) and (b) show that the convergence speed of the ANSGA-II algorithm is faster than that of NSGA-II. It tends to converge after about 50 iterations and is less likely to fall into local optima.

To demonstrate the solution performance more intuitively, the Pareto front obtained by ANSGA-II is compared with NSGA-II, as exhibited in Fig.11. Comparing Figure11 (a) and (b), in comparison to NSGA-II, the Pareto optimal frontier obtained by ANSGA-II has higher quality and can approach the real Pareto frontier very well. Therefore, the proposed ANSGA-II has high value in MOP solving.

To further validate the superiority of the ANSGA-II, its HV value evolution trajectory is compared with the Multi-objective Squirrel Search Algorithm (MOSSA) and NSGA-III, as shown in Figure 12. In Figure 12 (a), in the FMk02 example, the HV index of the ANSGA-II is consistently higher than MOSSA and NSGA-III. In Figure 12 (b), in the FMk06 example, the improved algorithm still has the highest HV index. The Pareto front obtained by ANSGA-II covers a wide range in the target space and has certain advantages.

To more intuitively demonstrate the performance differences of different algorithms at specific time points or conditions, the IGD indicators of the three algorithms are compared, and the results are shown in Figure 13. Figure 13 shows that the IGD index of ANSGA-II algorithm is consistently lower than that of traditional NSGA-II and MOSSA, indicating better convergence and distribution performance.
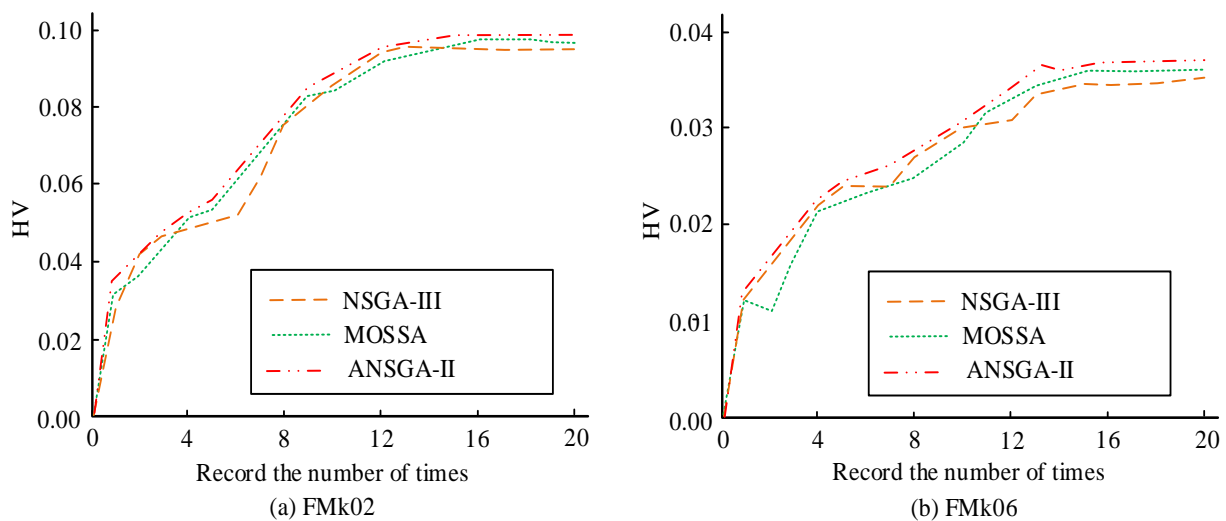

(a) FMk02

(b) FMk06

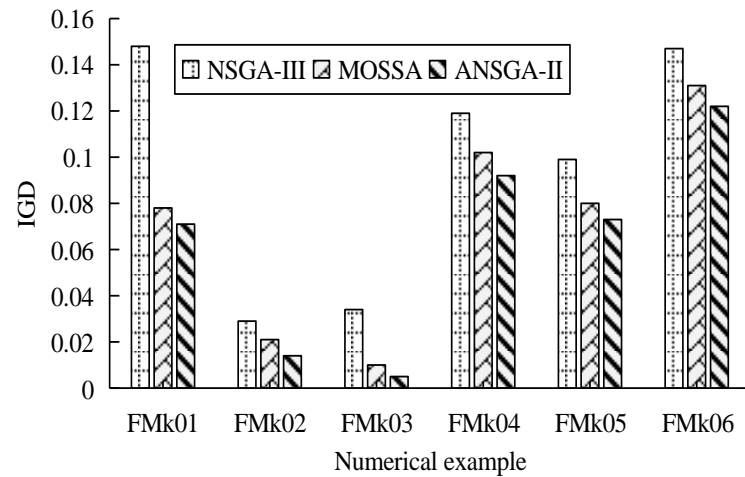Figure 12: Comparison results of indicators for three algorithms.

Figure 13: Comparison of IGD indicators for three algorithms.

To further verify the superiority of the ANSGA-II algorithm, its IGD index is compared with the more advanced improved NSGA-II algorithm proposed by Jalili A A [25], Zhang F [26], and Wang J [27], and the results are shown in Table 5. Table 5 shows that the IGD index of the proposed ANSGA-II algorithm is consistently lower than that of the improved NSGA-II algorithm proposed by Jalili A A [25], Zhang F [26], and Wang J [27] in FMk01-06. This indicates that the convergence of the ANSGA-II algorithm has certain superiority.

Table 5: Comparison of IGD indicators for four algorithms.

Numerical example	Algorithm			
	Jalili A A[25]	Zhang F[26]	Wang J[27]	ANSGA-II
FMk01	0.082	0.076*	0.079	0.071*@
FMk02	0.023	0.017*	0.021	0.014*@
FMk03	0.015	0.009*	0.011	0.005*@
FMk04	0.104	0.096*	0.102	0.092*@
FMk05	0.081	0.078*	0.078	0.073*@
FMk06	0.137	0.125*	0.134	0.122*@

Note: * indicates significant difference compared to the method in reference [25]; # indicates significant difference compared to the method in reference [26]; @ indicates significant difference compared to the method in reference [27], $p < 0.05$.

4   Discussion

This study proposed an ANSGA-II algorithm. In the experiment, the overall performance of the ANSGA-II in IGD and C-metric indicators was superior to traditional NSGA-II and MOEA/D. In the ZDT6 function, the proposed algorithm had a C-metric of 0, while the other two algorithms had a C-metric of 1. On ZDT2, the proposed algorithm obtained a high-quality Pareto optimal frontier, which could effectively approximate the true Pareto frontier. In DTLZ1, as the number of targets increased, the IGD of the algorithm showed a gradually increasing trend. The IGD of ANSGA-II algorithm did not exceed 2, and the IGD index in DTLZ2 did not exceed 1. In different examples, the HV index of the proposed algorithm was higher than that of NSGA-II, with the highest HV value of 0.098 in FMk02. The IGD of the proposed algorithm was lower than that of NSGA-II, with the lowest IGD value of 0.009 in FMk03.

In terms of convergence speed and diversity, the ANSGA-II algorithm can better approximate the true Pareto front on the ZDT series functions because the AC and mutation operators can dynamically adjust parameters according to the evolutionary state of the population, making the algorithm more efficient in exploring the solution space during the search process. In addition, crossover operators based on normal distribution can generate new individuals according to the distribution of the population, making the solution set more diverse. However, the convergence speed of the traditional NSGA-II algorithm is relatively slow, and it maintains population diversity through the crowding distance operator. In some cases, there may be issues with uneven individual distribution, leading to insufficient solution diversity. MOEA/D improves convergence speed while maintaining population diversity through decomposition strategies and neighborhood mechanisms. However, its solution set distribution on certain test functions may not be as uniform as the proposed ANSGA-II, such as ZDT6. In terms of computational efficiency, due to the introduction of adaptive strategies and crossover operators based on normal distribution, the ANSGA-II algorithm can reduce unnecessary calculations to a certain extent and improve the running efficiency of the algorithm. The

computational complexity of NDS in traditional NSGA-II is relatively high. However, the ANSGA-II algorithm requires evaluating and analyzing the state of the population during each iteration to determine the adjustment method and magnitude of parameters, which will increase certain computational overhead.

The actual industrial environment is often full of uncertainty, requiring real-time adjustment of strategies, and often requiring simultaneous optimization of multiple conflicting objectives. The ANSGA-II algorithm proposed by the research institute has good adaptability to dynamic environments and MOO capabilities, making it significantly advantageous in industrial scheduling problems such as logistics management and workshop scheduling. It can effectively solve complex MOPs and maintain efficient performance in dynamic environments. Future research can further expand its applications in other industrial fields, such as manufacturing, logistics, and energy management.

5   Conclusion

To effectively solve MOP, this study proposed an ANSGA-II algorithm and models the multi-objective FJSS problem by combining worker fatigue factors. Finally, the performance and MOO effect of the proposed algorithm were validated in ZDT series test functions, DTLZ series test functions, and FMk examples. The main findings of this study include: (1) Adaptive strategies can dynamically adjust the parameters of crossover and mutation operators, improving the algorithm's global and local search capabilities. (2) The crossover operator based on normal distribution can generate offspring individuals with more uniform distribution, enhancing the spatial search ability of the algorithm. In summary, the proposed ANSGA-II effectively solves MOPs. However, the running speed of the ANSGA-II algorithm in large-scale MOPs still needs to be further improved. Therefore, in future research, measures to improve the efficiency of the NSGA-II algorithm should be further explored. For example, NSGA-II algorithm components can be executed in parallel using multiple threads or processors, or feature extraction and dimensionality reduction can be achieved by integrating machine learning algorithms to reduce the complexity and computational overhead of NSGA-II operations.

References

[1]   Binoy Krishna Giri, and Sankar Kumar Roy. Neutrosophic multi-objective green four-dimensional fixed-charge transportation problem. International Journal of Machine Learning and Cybernetics, 13(10):3089-3112, 2022.https://link.springer.com/article/10.1007/s130 42-022-01582-y

[2]   Joydeep Dutta, Partha Sarathi Barma, Anupam Mukherjee, Samarjit Kar, and Tanmay De. A hybrid multi-objective evolutionary algorithm for open vehicle routing problem through cluster primary-route secondary approach. International Journal of Management Science and Engineering Management, 17(2):132-146, 2022.https://doi.org/10.1080/17509653.2021.20009 01

[3]   Shubhkirti Sharma, and Vijay Kumar. A comprehensive review on multi-objective optimization techniques: Past, present and future. Archives of Computational Methods in Engineering, 29(7):5605-5633, 2022.https://link.springer.com/content/pdf/10.1007/ s11831-022-09778-9.pdf

[4]   Wu Deng, Xiaoxiao Zhang, Yongquan Zhou, Yi Liu, Xiangbing Zhou, Huiling Chen, and Huimin Zhao. An enhanced fast non-dominated solution sorting genetic algorithm for multi-objective problems. Information Sciences, 585(11):441-453, 2022.https://doi.org/10.1016/j.ins.2021.11.052

[5]   Pradeep Jangir, Hitarth Buch, Seyedali Mirjalili, and Premkumar Manoharan. MOMPA: Multi-objective marine predator algorithm for solving multi-objective optimization problems. Evolutionary Intelligence, 16(1):169-195, 2023.https://doi.org/10.1007/s12065-021-00649-z

[6]   Sushmita Sharma, Nima Khodadadi, Apu Kumar Saha, Farhad Soleimanian Gharehchopogh, and Seyedali Mirjalili. Non-dominated sorting advanced butterfly optimization algorithm for multi-objective problems. Journal of Bionic Engineering, 20(2):819-843, 2023.https://link.springer.com/article/10.1007/s422 35-022-00288-9

[7]   Chang Liu, Jin Wang, Liang Zhou, and Amin Rezaeipanah. Solving the multi-objective problem of IoT service placement in fog computing using cuckoo search algorithm. Neural Processing Letters, 54(3):1823-1854, 2022.https://link.springer.com/article/10.1007/s110 63-021-10708-2

[8]   Aamir Ali, Ghulam Abbas, Muhammad Usman Keerio, Mohsin Ali Koondhar, Kiran Chandni, and Sohrab Mirsaeidi. Solution of constrained mixed‑integer multi-objective optimal power flow problem considering the hybrid multi-objective evolutionary algorithm. IET Generation, Transmission & Distribution, 17(1):66-90, 2023.https://doi.org/10.1049/gtd2.12664

[9]   Kasin Ransikarbum, and Scott Jennings Mason. A bi-objective optimisation of post-disaster relief distribution and short-term network restoration using hybrid NSGA-II algorithm. International Journal of Production Research, 60(19):5769-5793, 2022.https://doi.org/10.1080/00207543.2021.19708 46

[10] LinGen Chen, HongWei Zhu, YanLin Ge, ShuangShuang Shi, and HuiJun Feng. Multi-objective constructal design for quadrilateral heat generation body based on thermal-entransy theory and NSGA-II. Science China Technological Sciences, 67(9):2777-2786, 2024.https://doi.org/10.1007/s11431-023-2587-5

[11] Lingling Lv, and Weiming Shen. An improved NSGA-II with local search for multi-objective integrated production and inventory scheduling problem. Journal of Manufacturing Systems, 68(3):99-116, 2023.https://doi.org/10.1016/j.jmsy.2023.03.002

[12] Ahmad Aman Jalili, Mohsen Najarchi, Saeid Shabanlou, and Reza Jafarinia. Multi-objective optimization of water resources in real time based on integration of NSGA-II and support vector machines. Environmental Science and Pollution Research, 30(6):16464-16475, 2023.https://link.springer.com/article/10.1007/s113 56-022-22723-4

[13] Manish Kumar Singh, Amit Choudhary, Sandeep Gulia, and Anurag Verma. Multi-objective NSGA-II optimization framework for UAV path planning in an UAV-assisted WSN. The Journal of Supercomputing, 79(1):832-866, 2023.https://doi.org/10.1007/s11227-022-04701-2

[14] Lan Chen, Ling-ling Cao, Yao-min Wen, Hongsheng Chen, and Sheng-Long Jiang. A knowledge-based NSGA-II algorithm for multi-objective hot rolling production scheduling under flexible time-of-use electricity pricing. Journal of Manufacturing Systems, 69(6):255-270, 2023.https://doi.org/10.1016/j.jmsy.2023.06.009

[15] Jiabing Wang, Linlang Zeng, and Kun Yang. Multi-objective optimization of printed circuit heat exchanger with airfoil fins based on the improved PSO-BP neural network and the NSGA-II algorithm. Nuclear Engineering and Technology, 55(6):2125-2138, 2023.https://doi.org/10.1016/j.net.2023.02.029

[16] Haixia Chen. Optimization of production scheduling in the process industry using decomposed multi-objective evolutionary algorithms. Informatica, 48(22):85-97, 2024.https://doi.org/10.31449/inf.v48i22.6369

[17] Yanlu Gong, Junhai Zhou, Quanwang Wu, MengChu Zhou, and Junhao Wen. A length-adaptive non-dominated sorting genetic algorithm for Bi-objective high-dimensional feature selection. IEEE/CAA Journal of Automatica Sinica, 10(9):1834-1844, 2023.https://doi.org/10.1109/JAS.2023.123648

[18] Dai Tho Dang, Ngoc Thanh Nguyen, and Dosam Hwang. Hybrid genetic algorithms for the determination of DNA motifs to satisfy postulate 2-Optimality. Applied Intelligence, 53(8):8644-8653, 2023.https://doi.org/10.1007/s10489-022-03491-7

[19] Guojiang Xiong, Xufeng Yuan, Ali Wagdy Mohamed, Jun Chen, and Jing Zhang. Improved binary gaining-sharing knowledge-based algorithm with mutation for fault section location in distribution networks. Journal of Computational Design and Engineering, 9(2):393-405, 2022.https://doi.org/10.1093/jcde/qwac007

[20] Jose L. Carles-Bou and Severino F. Galán. Self-adaptive polynomial mutation in NSGA-II. Soft Computing, 27(23):17711-17727, 2023.https://doi.org/10.1007/s00500-023-09049-0

[21] Juan José Moreno, Savíns Puertas-Martín, Juana L. Redondo, Pilar M. Ortigosa, Anna Zawadzka, Pawel Kukołowicz, Robert Szmurio, Ignacy Kaliszewski, Janusz Miroforidis, and Ester M. Garzón. Bi-level optimization to enhance intensity modulated radiation therapy planning. Informatica, 36(1):99-124, 2025.https://doi.org/10.48550/arXiv.2311.10272

[22] Srila Dey, Florentin Smarandache, Rama Debbarma, and Priyanka Majumder. A hybrid IF-FUCOM-GRA approach and its application to determine optimal bacterial concentrations on mortar at optimal curing day. Informatica, 34(2):223-248, 2023. https://doi.org/10.15388/22-INFOR504

[23] Nurhan Dudaklı and Adil Baykasoglu. Performance evaluation of different dispatching rules and heuristics in a fully automated parking system. Informatica, 35(1):99-129, 2024.https://doi.org/10.15388/24-INFOR544

[24] Weihua Tan, Xiaofang Yuan, Jinlei Wang, and Xizheng Zhang. A fatigue-conscious dual resource constrained flexible job shop scheduling problem by enhanced NSGA-II: An application from casting workshop. Computers & Industrial Engineering, 160(1-17):107557, 2021.https://doi.org/10.1016/j.cie.2021.107557

[25] Ahmad Aman Jalili, Mohsen Najarchi, Saeid Shabanlou, and Reza Jafarinia. Multi-objective optimization of water resources in real time based on integration of NSGA-II and support vector machines. Environmental Science and Pollution Research, 30(6):16464-16475, 2023.https://doi.org/10.1007/s11356-022-22723-4

[26] Fushun Zhang. Constructing a multi-objective optimization model for engineering projects based on NSGA-II algorithm under the background of green construction. Decision Making: Applications in Management and Engineering, 7(1):37-53, 2024.https://doi.org/10.31181/dmame712024895

[27] Jiabing Wang, Linlang Zeng, and Kun Yang. Multi-objective optimization of printed circuit heat exchanger with airfoil fins based on the improved PSO-BP neural network and the NSGA-II algorithm. Nuclear Engineering and Technology, 55(6):2125-2138, 2023.https://doi.org/10.1016/j.net.2023.02.029